SCIENCE CHINA
Technological Sciences

• Article •

January 2023 Vol.66 No.1: 000000
doi: 10.1007/s11433-000-0000-0

Hydrogen generation from the spontaneous reaction of water, CO_2, and Martian meteorites

TANG XuHai[1], ZHANG YiHeng[1], QIAO JiangMei[1], ZHAO YuYan Sara[2], HUANG LiZhi[1*], LIU YiWei[1*]

[1]*School of Civil Engineering, Wuhan University, Wuhan 430072, China;*
[2] *International Center for Planetary Science, College of Geosciences, Chengdu University of Technology, Chengdu 610059, China*

Received January 1, 2023; accepted January 1, 2023; published online January 1, 2023

Understanding the interaction of Martian rocks and environment is conducive to the Mars In Situ Resource Utilization (ISRU) and searching for natural H_2 reservoirs. Here, we report an interesting finding: for the first time, using a real Martian meteorite (NWA13190) and within Mars' temperature range (25°C), we confirmed spontaneous hydrogen generation from the reaction of water, CO_2, and Martian rock—no external energy or catalysts required. The reaction produced hydrogen at ~4 ppm/day, stabilizing after 9 days, alongside newly formed carbonate and sulfate minerals absent in the original meteorite. Mechanistic analyses using XPS, Mössbauer spectroscopy, and FTIR revealed that Fe^{2+} in $FeTiO_3$ and FeS_2 (not pyroxene) oxidized to Fe^{3+}, driving water reduction to hydrogen. The buffer effect of CO_2 sustained acidic conditions, enhancing Fe^{2+} release and H2 production. These results align with in-situ Mars detections (e.g., Ca-sulfate veins by Curiosity). Compared to energy-intensive electrolysis-based ISRU, this geological process offers a more efficient H_2 production pathway. It also provides theoretical support for natural hydrogen reservoirs on Mars and simultaneously advances understanding of Mars' early atmospheric evolution and potential life-supporting environments.

hydrogen generation, water-CO_2-Martian rock reaction, in situ resource utilization

Citation: Tang X H, Zhang Y H, Qiao J M, et al. Hydrogen generation from the spontaneous reaction of water, CO_2, and Martian meteorites. Sci China Tech Sci, 2026, 59: 183–190, doi: 10.1007/s11431-015-5920-2

1 Introduction

The atmosphere of Mars is primarily composed of CO_2, accounting for about 95.32% of its total volume. The remaining elements include nitrogen (2.7%), argon (1.6%), water vapor (0.03%), and other gases. Additionally, water exists on Mars in the form of ice, particularly at the polar ice caps, but also beneath the surface across much of the planet, even in some near-equatorial regions [1]. Enhancing our understanding of the interaction of water, CO_2, and Martian rocks (the reaction of water-CO_2-MR) is conducive to many fields, including Mars In Situ Resource Utilization (ISRU), providing clues of hydrogen-based microbial life, investigating geological history, and searching for natural hydrogen resources.

The ISRU is crucial for long-term Mars missions, which seem to be viable and cost effective. For Mars, potential ISRU resources include CO_2 in the atmosphere, water ice in the subsurface, and various minerals in the Martian geomaterials. In 2020, the Mars Oxygen In-Situ Resource Utilization Experiment (MOXIE), a component of NASA' s Mars Perseverance rover, successfully produced oxygen (O_2) from CO_2 in the Martian atmosphere as part of an ongoing experiment [2]. Various studies of Mars missions have suggested using indigenous resources to manufacture rocket

*Corresponding author (email: liuyiwei@whu.edu.cn; lizhihuang@whu.edu.cn)

propellant for the ascent vehicle that will lift a crew off the surface of Mars. A widely researched and practical method, known as the Sabatier-Electrolysis process, is available for producing methane (CH_4) and O_2 from CO_2 and hydrogen (H_2). Therefore, the problem for this process on Mars is obtaining H_2. Gayen et al. (2020) [3] realized the concurrent production of hydrogen fuel and life-support oxygen on Mars through perchlorate brine electrolysis. However, the electrolysis needs extra electric energy input and complex electrocatalysts [4]. The successful reaction of water, CO_2, and Martian rocks provides potential geological technology for producing giant hydrogen without any extra energy input or catalysts. Additionally, the water-CO_2-MR reaction provides a theoretical basis for the possibility of searching for the natural hydrogen reservoir within Mars. On Earth, recent discoveries have unearthed a bonanza of natural geological hydrogen in significantly larger quantities than previously thought possible; therefore, recently searching for hydrogen naturally produced within Earth has attracted intensive attention [5,6]. The feasibility of in-situ hydrogen production in underground environments, such as basalt formations, oil and gas reservoirs, has recently attracted growing research interest [7, 8].

Understanding the interaction between CO_2, water, and Martian geomaterials is critical for us to understand the significant geological and atmospheric changes of Mars throughout its 4.6-billion-year history. The presence of valleys on ancient terrains of Mars suggests that liquid water flowed on the Martian surface 3.8 Gyr ago or before [9]. The above-freezing temperatures required to explain valley formation could have been transient, in response to the frequent large meteorite impacts on early Mars, or they could have been caused by long-lived greenhouse warming [10,11]. Currently, reconciling the geology of Mars with models of atmospheric evolution remains a major challenge [12]. Additionally, understanding the hydrogen-related geological evolution on Mars potentially helps us to search for hydrogen-based microbial life. By producing hydrogen from the reaction of water and Earth's mafic and ultramafic rocks at 55°C, Mayhew et al. (2013) [13] point out that the localized sites of hydrogen generation in Martian rocks could support hydrogen-based microbial life.

Previous researches have produced hydrogen from lab-synthesized materials or Earth minerals/rocks [14,15]. However, there is still a lack of investigation based on real Martian rocks, temperature, and atmosphere. Mayhew et al. (2013) [13] reacted Earth's mafic and ultramafic rocks with water to produce H_2 at 55°C, and this temperature exceeds the temperature on Mars, ranging from −133°C to 27°C. In contrast, our experimental results showed that hydrogen gas was not produced from the reaction between water and the Martial meteorite at 25°C in the absence of CO_2. Additionally, we found that the presence of CO_2 triggers the reaction of water and Martian meteorites to produce hydrogen, and the reaction temperature can be reduced to as low as 25°C.

In this work, the experiments present two original novelties: (1) the starting material is real Martian rocks rather than lab-synthesized materials or natural minerals on Earth; (2) the hydrogen production reaction was carried out at 25°C, which is within the Martian temperature range from −133°C to 27°C. Our approach provides a unique pathway to fuel production for future human missions to Mars, to understand the early Martian atmosphere consisting of CO_2 and H_2.

2 Materials and methods

The Martian meteorite sample used in this study is Northwest Africa 13190 (NWA13190), which exhibits a weathered fusion crust on the exterior, while the interior remains fresh (Figure 1a). To ensure experimental integrity, only the unaltered interior portion was used, avoiding both the weathered crust and shock-melt veins. The mineralogical composition of NWA13190 prior to reaction with the water-CO_2-meteorite (water-CO_2-MR) system was determined using a TESCAN Integrated Mineral Analyzer (TIMA), while the chemical composition and formulas of individual minerals were obtained via electron microprobe analysis (EMPA) (see supplementary materials Table S1)[16]. NWA13190 is classified as a shergottite, which is one of the most common and compositionally diverse subgroups of Martian meteorites. EMPA shows that the martian meteorite contains pigeonite, maskelynite, subcalcic augite, Si-Al-K-Na-rich glass, merrillite, titanomagnetite, and troilite.

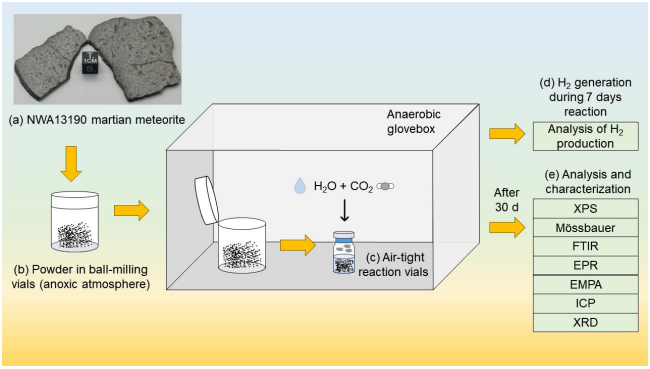

Figure 1 The experimental setup for the water-CO_2-MR reaction. (a) NWA13190 Martian meteorite; (b) ball milling in ball-milling vials at anoxic atmosphere; (c) carry out water-CO_2-MR reaction in air-tight reaction vials in anaerobic glovebox; (d) H_2 was monitored during 11 days reaction; (e) analysis and characterization after 30 days.

To investigate hydrogen generation during the water-CO_2-MR reaction, all experiments were conducted in an oxygen-free glovebox filled with high-purity nitrogen gas (99.999%), maintaining O_2 levels below 0.1 ppm. The

meteorite was first pulverized into fine powder by ball milling to enhance its surface area and reaction kinetics. Specifically, 2.0 g of meteorite and forty zirconia balls (0.6 cm diameter) were placed into milling vials inside the glovebox (Figure 1b), which were then sealed and removed for ball milling at 450 rpm for 20 hours. The ball-milled powder was transferred to airtight reaction vessels containing CO_2-saturated ultrapure water and a CO_2 headspace (Figure 1c). Two types of experiments were conducted: a long-term (11-day) test in a 450 mL reactor (100 mL water, 2 g Martian rock), and a short-term (1-day) test in a 10 mL reactor (5 mL water, 0.1 g Martian rock). Hydrogen production was monitored over 11 days, with experiments repeated in duplicate for each time point (t = 1 to 11 days). At each time t, 1 mL of headspace gas was withdrawn using a gas-tight syringe and analyzed immediately using a gas chromatograph (GC-7890B, Agilent) equipped with a high-sensitivity thermal conductivity detector (TCD) (Figure 1d).

To further evaluate reaction extent, a 30-day experiment was conducted. After the reaction, solid samples were collected by centrifugation, dried in the glovebox, and subjected to multi-technique characterizations (Figure 1e). The chemical states of elements were analyzed using X-ray photoelectron spectroscopy (XPS, ESCALAB250Xi, Thermo VG Scientific, USA), calibrated using the C1s peak at 284.80 eV. Iron valence states (Fe^{2+}/Fe^{3+}) were determined by Mössbauer spectroscopy, and functional groups were identified using Fourier Transform Infrared Spectroscopy (FTIR). Oxygen vacancies were assessed via Electron Paramagnetic Resonance (EPR), while mineralogical changes were examined using TIMA, EMPA, and X-ray diffraction (XRD). Ion concentrations in the leachate were measured using Inductively Coupled Plasma Optical Emission Spectroscopy (ICP-OES).

3 Results

3.1 Hydrogen production

Figure 2a shows that the Martian meteorite produced H_2 in CO_2-saturated water at a pseudo-zero-order rate of ~4 ppm/day, with production plateauing after 9 days. This equals $5.8-9.1\times10^{-8}$ g H_2 production per gram of Martian regolith per day under the experimental conditions (values account for the pressure of the CO_2 headspace). As shown in Figure 2b, H_2 was not generated in the absence of either CO_2 (Figure 2b II) or meteorite (Figure 2b III), indicating that both the Martian meteorite and CO_2 are essential for hydrogen generation. The pH of CO_2-saturated water is approximately 3.3, which facilitated the release of 3 mM Fe^{2+} ions from Martian meteorites. A similar amount of H_2 was obtained when the same concentration of Fe^{2+} was externally added without CO_2 (Figure 2b I and IV), highlighting the role of Fe^{2+} at the rock–water interface in promoting H_2 generation. In contrast, Fe^{2+} alone in acidic water did not produce H_2, consistent with our previous studies [17].

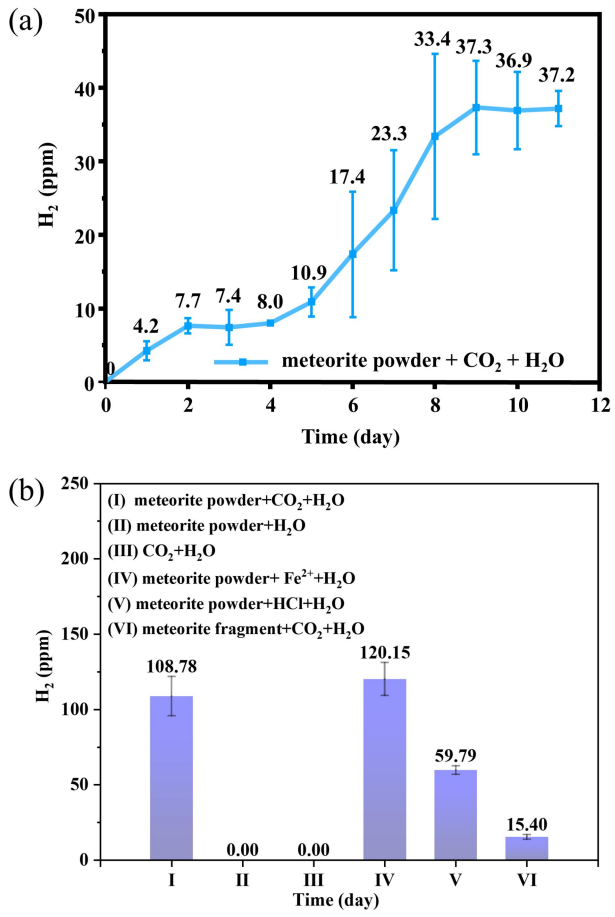

Figure 2 H_2 generation from the water-CO_2-MR reaction. (a) H_2 generation for 11 days reaction with meteorite powder in CO_2-saturated aqueous solution (in 450 mL reactors). (b) H_2 generation after 1 day of reaction in different systems (in 10 mL reactors). (I) meteorite powder in CO_2-saturated aqueous solution, (II) meteorite powder in aqueous solution at pH 11, (III) CO_2-saturated aqueous solution without meteorite, (IV) meteorite powder in aqueous solution with the addition of extra ~3 mM of Fe^{2+} ions, (V) meteorite powder in HCl aqueous solution, (VI) meteorite fragments in CO_2-saturated aqueous solution. Experimental conditions: ~3 mM of Fe^{2+} was released in (I), and the same concentration of Fe^{2+} was added to (IV). The pH values of (I) and (V) are both ~3.3. The pH value of (IV) is ~6.4.

To isolate pH effects, the meteorite suspension was adjusted to pH ~3.3 using HCl, releasing only 0.5 mM Fe^{2+} and producing ~60 ppm H_2—much less than in the CO_2 system—due to reduced Fe^{2+} availability. Final pH was higher in the HCl system (5.9 vs. 5.5), indicating that the CO_2 buffer better sustained acidic conditions, enhancing Fe^{2+} release and H_2 production.

Lastly, using crushed meteorite fragments (instead of ball-milled powder) led to only 15.4 ppm H_2 after 24 h, ~14% of the yield from the ball-milled sample, confirming

that a larger surface area significantly promotes H_2 generation.

3.2 Fe^{2+}/Fe^{3+} analysis in meteorites by XPS

XPS spectra before and after reaction revealed characteristic peaks of Mg, Na, Fe, O, Ca, C, Si, and Al (Figure 3). Post-reaction decreased Na and Ca signals suggest dissolution of corresponding minerals. The C=O peak increased from 6.96% to 16.58%, indicating carbonate formation via CO_2 fixation, consistent with EMPA results (Figure 3b). Fe 2p peaks confirm partial oxidation of Fe^{2+} (709.9 eV) to Fe^{3+} (711.4 eV), with Fe^{3+} content increasing from 39.46% to 41.22% and Fe^{2+} decreasing from 22.01% to 17.17% (Figure 3c). Mg and Si spectra remained unchanged, indicating their limited involvement. Overall, the results suggest H_2 generation is associated with Fe^{2+} oxidation at the meteorite surface.

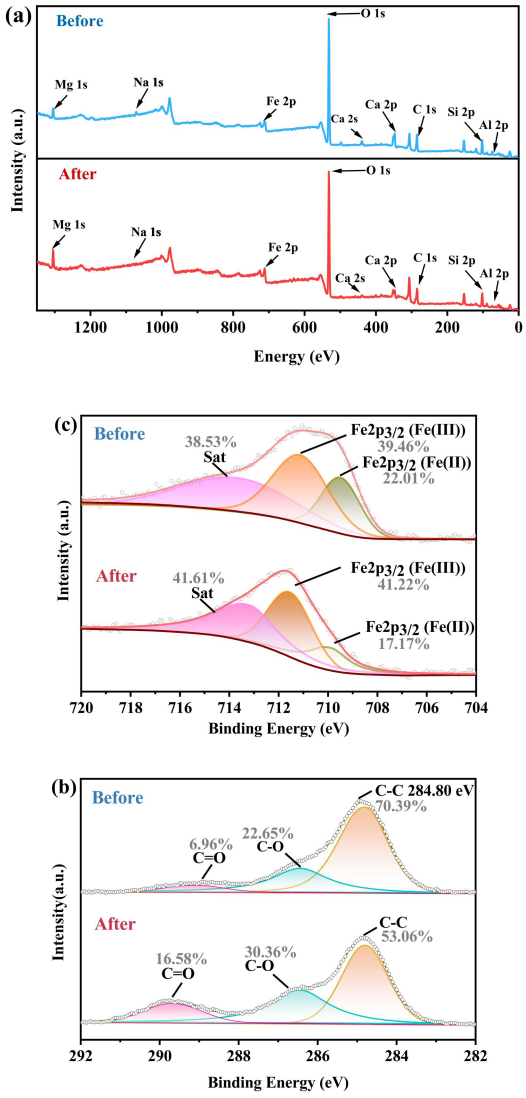

Figure 3 XPS of Martian meteorite before and after reaction. (a) XPS survey, (b) C 1s, (c) Fe 2p.

3.3 Fe-bearing phase in minerals by Mössbauer spectroscopy

Mössbauer analysis showed stable Fe^{2+} content in pyroxene before and after reaction, indicating its inactivity in H_2 production. In contrast, Fe^{2+} in $FeTiO_3$ and FeS_2 was oxidized to octahedrally coordinated Fe^{2+}, as evidenced by the appearance of a new ferric doublet and increased quadrupole splitting, confirming structural transformation during redox processes. The results are shown in the Supporting Information.

3.4 Functional groups changes by FTIR

As shown in Figure 4, FTIR spectra revealed stronger OH (H-O-H bend) stretching bands at 3419 cm^{-1} and 3430 cm^{-1} after reaction, suggesting enhanced adsorption of water on the meteorite surface and the strengthened hydroxyl connectivity within the meteorite sample [18,19]. Increases in C=O (1504 cm^{-1}) and OH (1417 cm^{-1}) vibrations indicate surface carbonation [20,21]. Shifts in Si-O-Fe and Si-O-Si peaks (1024 cm^{-1} and 1031 cm^{-1}) may reflect secondary silicate formation, as confirmed by EMPA analysis (Table S1)[22]. Bands near 725 cm^{-1} (FeO_4), 630 cm^{-1} (Fe-OH), and 480 cm^{-1} (quartz) further support mineralogical changes induced by reaction [19,21,23].

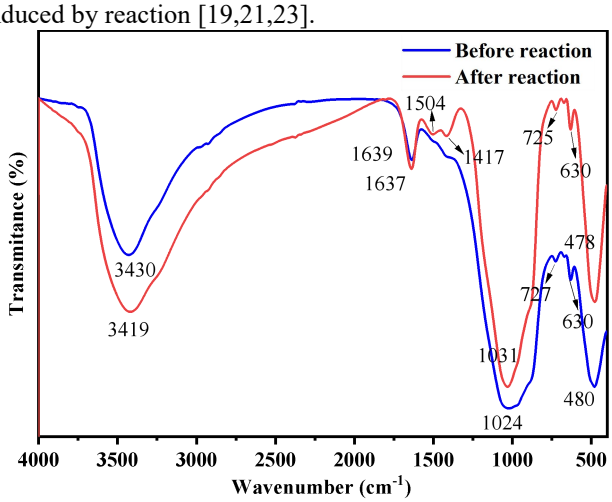

Figure 4 FTIR spectra of Martian meteorite before and after reaction.

3.5 Fe^{2+} release and pH evolution

Hydrogen generation in systems I, IV, V, and VI was accompanied by pH increases due to proton consumption (Table 1), consistent with previous studies [24–26]. CO_2 induced greater Fe^{2+} release than HCl, leading to higher H_2 production, confirming a direct correlation between Fe^{2+} concentration and H_2 yield. The modest pH shift in group IV reflects its initially higher pH. Overall, pH evolution is indicative of water reduction coupled with Fe^{2+} oxidation.

Table 1 Fe^{2+} release and pH change before and after reaction

Group	Fe^{2+} concentration (mM)	pH	
		Before reaction	After reaction
(I) meteorite powder + CO_2 + H_2O	3.0	3.3	5.5
(II) meteorite powder + H_2O	0.05	11	11
(III) CO_2 + H_2O	0	3.3	3.3
(IV) meteorite powder + Fe^{2+} + H_2O	3.0	6.4	6.5
(V) meteorite powder + HCl + H_2O	0.5	3.3	5.9
(VI) meteorite fragments + CO_2 + H_2O	0.09	3.3	4.2

3.6 Oxygen vacancy analysis by EPR

The EPR result revealed a consistent oxygen vacancy signal at g = 2.005 before and after reaction, attributed to surface defects [27,28]. However, the signal intensity decreased post-reaction, indicating a reduction in oxygen vacancy concentration. As oxygen vacancies are known to facilitate electron transfer and promote H_2 production [29], this result suggests their partial consumption during the water-CO_2-MR reaction.

3.7 Reaction-induced mineralogical changes

The mineralogical evolution of the Martian meteorite before and after the water-CO_2-MR reaction was investigated using TIMA, EMPA, and ICP analyses. Pre-reaction phases included pigeonite, maskelynite, subcalcic augite, and Si-Al-K-Na-rich glass. Post-reaction, new silicate minerals (e.g., $Fe_{1.976}Mg_{0.134}Ti_{0.040}Mn_{0.033}Cr_{0.002}Si_{0.887}O_4$), as well as carbonate and sulfate minerals that are not present initially, were identified by EMPA (Figure 5). ICP results revealed increased concentrations of Mn, Fe, Ni, Cu, Na, Mg, K, Ca, and Ba in leachates after reaction, attributed to acid-driven dissolution by carbonic acid. Subsequent precipitation of Mn, Fe, P, Mg, and Ca as carbonates, and Ba, Ca, Ti, Zn, and Fe as sulfates, aligns with observed mineral phases.

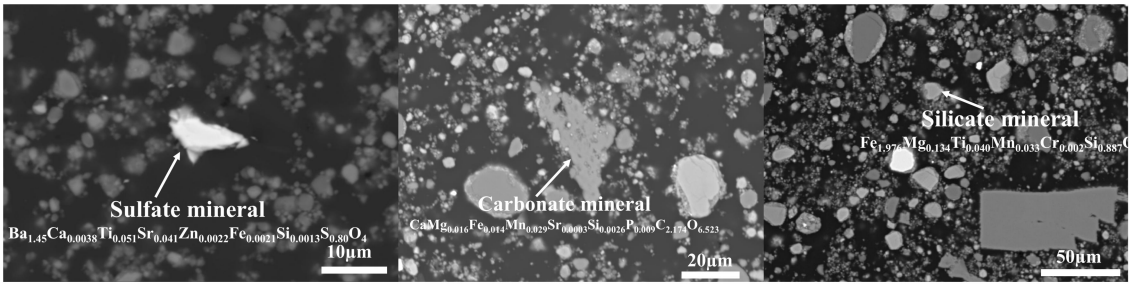

Figure 5 Backscattered electron (BSE) images of sulfate minerals, carbonate minerals, and new silicate minerals.

4 Discussions

The mechanism of H_2 generation is illustrated in Figure 6 and summarized in eqs. 1-4. Dissolved CO_2 forms carbonic acid (eq. 1), which promotes the dissolution of $FeTiO_3$ and FeS_2, releasing Fe^{2+} (eqs. 2-3), as confirmed by XPS and Mössbauer data. The released Fe^{2+} adsorbs onto the meteorite surface ($Fe^{2+}_{MR\text{-}surface}$), where it donates electrons to protons, generating H_2 (eq. 4). The increases in surface OH groups (FTIR) and pH further support proton consumption. These findings confirm that Fe^{2+} oxidation drives water reduction and H_2 generation, facilitated by surface electron transfer.

$$CO_2+H_2O\rightarrow H_2CO_3, \quad (1)$$

$$H_2CO_3+FeTiO_3\rightarrow Fe^{2+}+CO_3^{2-}+TiO_2+H_2O+CO_2\uparrow, \quad (2)$$

$$H_2CO_3+4FeS_2+8H_2O\rightarrow 4Fe^{2+}+8SO_4^{2-}+15H^++CO_2\uparrow, \quad (3)$$

$$2Fe^{2+}_{MR\text{-}surface}+2H^+_{MR\text{-}surface}\rightarrow 2Fe^{3+}_{MR\text{-}surface}+H_2\uparrow, \quad (4)$$

The present experimental results are consistent with some in-situ detection results on Mars. Martian meteorites, ejected from the underground due to impacts, may not have undergone the weathering process. Our experimental results reflect the water- and CO_2-related weathering processes on Mars involving interactions with liquid water and the atmosphere.

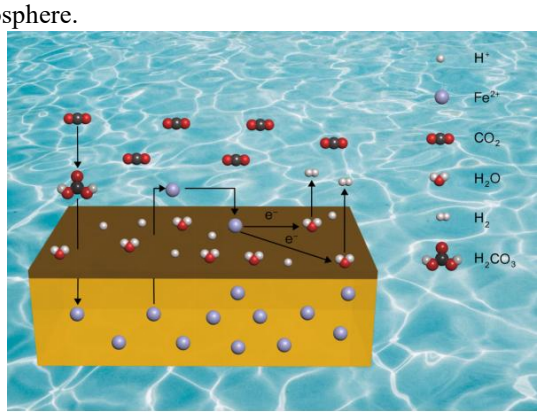

Figure 6 Schematic representation of MR-surface-promoted H_2 generation via water-CO_2-MR reaction.

As shown in Table S3, the water-CO_2-MR reaction leads to the generation of carbonate minerals and sulfate minerals, which were not found in the Martian meteorites before the reaction. According to previous in-situ detection results on Mars, groundwater played an important role in formation and diagenesis of clay minerals [30]. Noachian and Hesperian sediments include paleolake deposits with clays, carbonates, sulfates, and chlorides [31]. The Spirit rover encountered Mg/Fe/Ca carbonates in the Columbia Hills Comanche outcrop [32]. The samples, collected by the Curiosity rover from the Vera Rubin ridge (VRR) on Mount Sharp, contain feldspars, pyroxene, hematite, calcium sulfates, phyllosilicates, and X-ray amorphous material. The light-toned Ca-sulfate veins encountered by the Curiosity rover are abundant throughout VRR [33–35]. These in-situ results further support the presence of sulfate-forming aqueous reactions similar to those reproduced in this study.

In our experiment, the H_2 production reached a plateau after 9 days, with no continuous CO_2 supply (Figure 2a). Thermodynamically, the reaction is spontaneous under the experimental conditions (25°C, CO_2-saturated aqueous environment), meaning it can proceed without external energy input. Notably, however, reaction kinetics emerge as the primary limiting factor for H_2 production efficiency and longevity. This is directly evidenced by the plateau in H_2 production after 9 days (Figure 2a), where production ceased. This kinetic limitation is likely driven by the formation of passivating mineral layers and depletion of reactive Fe^{2+}. Creation of carbonate minerals and sulfate minerals may grow a coating on the meteorite's surface. These phases act as a physical barrier, reducing mass transport of H_2O and CO_2 to the underlying reactive Fe^{2+} sites and blocking the release of newly generated H_2. Besides, the meteorite's H_2-generating capacity is tied to its Fe^{2+} content. XPS results show that Fe^{2+} decreased from 22.01% to 17.17% after reaction. This depletion, combined with passivation, explains the plateau in H_2 production. While the Martian surface (low temperature and pressure) would further slow reaction rates compared to our experimental conditions, the same limiting factors would likely govern long-term H_2 generation from Martian regolith. For ISRU applications, this suggests that strategies to mitigate passivation or target regolith with higher reactive Fe^{2+} content could enhance H_2 production scalability.

5 Conclusions

This study demonstrates that H_2 can be generated through a spontaneous reaction between water, CO_2, and the NWA13190 Martian meteorite at 25°C, without the need for external energy or a catalyst. This finding underscores the potential significance of the Martian atmosphere, which is composed of 95.32% CO_2, in facilitating the natural production of H_2 from aqueous reactions with Martian rocks. It was found that Fe^{2+} in $FeTiO_3$ and FeS_2, rather than in pyroxene, is oxidized to promote water reduction to produce H_2. Concurrently, our experiments show the formation of carbonate and sulfate minerals—none of which were initially present in the meteorites—suggesting transformative mineralogical processes. These observations are in partial agreement with in-situ measurements on Mars, such as the Ca-sulfate veins detected by NASA's Curiosity rover. Notably, our results reveal a mechanism for generating substantial geological hydrogen that is more energy-efficient compared to the electrolysis typically employed in In-Situ Resource Utilization strategies, which require additional electricity and catalysts. Moreover, our findings lay a theoretical foundation for the existence of natural hydrogen reserves on Mars, providing a novel avenue for future exploration.

This work was financially supported by the National Natural Science Foundation of China (Grant No. 41807188, 42402285, 51978537, and 52270165), the Fundamental Research Funds for the Central Universities (2042021kf0201), and Start-up Fund for Distinguished Scholars, Wuhan University (1403–413100041, 1403–600460022).

Conflict of interest The authors declare that they have no conflict of interest.

1 Rapp D. Use of extraterrestrial resources for human space missions to moon or mars, Springer; 2013. doi.org/10.1007/978-3-319-72694-6
2 Hoffman J A, Hecht M H, Rapp D, et al. Mars oxygen ISRU experiment (MOXIE)—preparing for human mars exploration. Sci Adv, 2022, 8: 8636
3 Gayen P, Sankarasubramanian S, Ramani V K. Fuel and oxygen harvesting from Martian regolithic brine. Proc Natl Acad Sci, 2020, 117: 31685–31689
4 Zhu Q, Huang Y, Zhou D, et al. Automated synthesis of oxygen-producing catalysts from Martian meteorites by a robotic AI chemist. Nat Synth, 2024, 3: 319–328
5 Zgonnik V. The occurrence and geoscience of natural hydrogen: A comprehensive review. Earth-Science Rev, 2020, 203: 103140
6 Hand E. Hidden hydrogen: Does Earth hold vast stores of a renewable, carbon-free fuel? Science, 2023, 336: 630–636
7 Tackie-Otoo B N, Mahmoud M, Murtaza M, et al. An Integrated Experimental and Simulation Study for the Feasibility of Underground H_2 Production from Natural Gas Reservoirs. ACS omega, 2025, 10: 24510–24519
8 Huang L Z, Liu Q S, Steefel C, et al. Generating H_2 during the CO_2 sequestration in basalt formations. Geomechanics and Geophysics for Geo-Energy and Geo-Resources, 2025, 11: 4
9 Carr M H. The Martian drainage system and the origin of valley networks and fretted channels. J Geophys Res Planets, 1995, 100: 7479–7507
10 Jakosky B M, Haberle R M, Arvidson R E. The changing picture of volatiles and climate on Mars. Science, 2005, 310: 1439–1440
11 Ramirez R M, Kopparapu R, Zugger M E,et al. Warming early Mars with CO_2 and H_2. Nat Geosci, 2014, 7: 59–63
12 Wordsworth R, Knoll A H, Hurowitz J, et al. A coupled model of episodic warming, oxidation and geochemical transitions on early Mars. Nat Geosci, 2021, 14: 127–132

13 Mayhew L E, Ellison E T, McCollom T M, et al. Hydrogen generation from low-temperature water--rock reactions. Nat Geosci, 2013, 6: 478–484
14 Osselin F, Pichavant M, Champallier R, et al. Reactive transport experiments of coupled carbonation and serpentinization in a natural serpentinite. Implication for hydrogen production and carbon geological storage. Geochim Cosmochim Acta, 2022, 318: 165–189
15 Wang J, Watanabe N, Okamoto A, et al. Pyroxene control of H_2 production and carbon storage during water-peridotite-CO_2 hydrothermal reactions. Int J Hydrogen Energy, 2019, 44: 26835–26847
16 Liu Y W, Zhang G P, Qiao J M, et al. Micromechanical testing and property upscaling of planetary rocks: A critical review. Int J Min Sci Techno, 2024, 34: 1217-1241
17 Jia Q Q, Deng J, Zhang X, et al. Hydroxyl groups bridge the electron transfer from Fe (II) to carbon tetrachloride. Water Res, 2022, 221: 118791
18 Omran M, Fabritius T, Elmahdy A M, et al. XPS and FTIR spectroscopic study on microwave treated high phosphorus iron ore. Appl Surf Sci, 2015, 345: 127–140
19 Lakshmi Reddy S, Udayabashakar Reddy G, Ravindra Reddy T, et al. XRD, TEM, EPR, IR and nonlinear optical studies of yellow ochre. J Laser Opt Photonics, 2015, 2: 120
20 Mehdilo A, Irannajad M. Comparison of microwave irradiation and oxidation roasting as pretreatment methods for modification of ilmenite physicochemical properties. J Ind Eng Chem, 2016, 33: 59–72
21 Nascimento-Dias B L, Zucolotto M E, Belgo H C, et al. Detection of organic or inorganic material in Martian meteorite Zagami by vibrational spectroscopy? Int J Astrobiol, 2020, 19: 438–445
22 Madejová J. FTIR techniques in clay mineral studies. Vib Spectrosc, 2003, 31: 1–10
23 Ciżman A, Rysiakiewicz-Pasek E, Antropova T, et al. Effect of the iron content on the structure and electrical properties of sodium borosilicate glasses: XRD, TEM, Mössbauer, FTIR and DIS spectroscopy study. J Non Cryst Solids, 2020, 531: 119847
24 McCollom T M, Klein F, Solheid P, et al. The effect of pH on rates of reaction and hydrogen generation during serpentinization. Philos Trans R Soc A, 2020, 378: 20180428.
25 Miller H M, Mayhew L E, Ellison E T, et al. Low temperature hydrogen production during experimental hydration of partially-serpentinized dunite. Geochim Cosmochim Acta, 2017, 209: 161–183
26 Santos J L, López E R, Ivanova S, et al. Low CO_2 hydrogen streams production from formic acid through control of the reaction pH. Chem Eng J, 2023, 455: 140645
27 Kesharwani N, Chaudhary N, Haldar C. Synthesis and characterization of Merrifield resin and graphene oxide supported air stable oxidovanadium (IV) radical complexes for the catalytic oxidation of light aliphatic alcohols. Catal Today, 2022, 397: 604–617
28 Jung J, Lee M-J. EPR investigation on the efficiency of hydroxyl radical production of gamma-irradiated anatase and bentonite. Water Res, 2002, 36: 3359–3363
29 Zhu K, Shi F, Zhu X, et al. The roles of oxygen vacancies in electrocatalytic oxygen evolution reaction. Nano Energy, 2020, 73: 104761
30 Ehlmann B L, Edwards C S. Mineralogy of the Martian surface. Annu Rev Earth Planet Sci, 2014, 42: 291–315
31 Ehlmann B L, Mustard J F, Fassett C I, et al. Clay minerals in delta deposits and organic preservation potential on Mars. Nat. Geosci, 2008, 1: 355–358
32 Morris R V, Ruff SW, Gellert R, et al. Identification of carbonate-rich outcrops on Mars by the Spirit rover. Science, 2010, 329: 421–424
33 L'Haridon J, Mangold N, Meslin P-Y, et al. Chemical variability in mineralized veins observed by ChemCam on the lower slopes of Mount Sharp in Gale crater, Mars. Icarus, 2018, 311: 69–86
34 Rampe E B, Bristow T F, Morris R V, et al. Mineralogy of Vera Rubin ridge from the Mars science laboratory CheMin instrument. J Geophys Res Planets, 2020, 125: e2019JE006306
35 McAdam A C, Sutter B, Archer P D, et al. Constraints on the mineralogy and geochemistry of Vera Rubin ridge, Gale crater, Mars, from Mars Science Laboratory Sample Analysis at Mars evolved gas analyses. J Geophys Res Planets, 2020, 125: e2019JE006309